学位論文

Intravital imaging of neutrophil recruitment in intestinal ischemia-reperfusion injury

（小腸虚血再灌流障害時における好中球動態の生体内イメージング）

橋本　晋太朗

Shintaro　Hashimoto

指導教員

猪股　裕紀洋　前教授

熊本大学大学院医学教育部博士課程医学専攻小児外科学・移植外科学

紹介教授

日比　泰造　　教授

熊本大学大学院医学教育部博士課程医学専攻小児外科学・移植外科学

2018年度

学　位　論　文

Doctoral Thesis

論文題名　: Intravital imaging of neutrophil recruitment in intestinal ischemia-reperfusion injury
（小腸虚血再灌流障害時における好中球動態の生体内イメージング）

著 者 名　:　橋本　晋太朗
（単名）　Shintaro　Hashimoto

指導教員名　:　熊本大学大学院医学教育部博士課程医学専攻小児外科学・移植外科学
猪股　裕紀洋　前教授

審査委員名　:

機能病理学　担当教授	伊藤　隆明
腎臓内科学　担当教授	向山　政志
国際先端医学研究機構　担当教授	滝澤　仁
免疫学　担当講師	粟井　博丈

２０１８年度

Biochemical and Biophysical Research Communications 495 (2018) 2296–2302

Contents lists available at ScienceDirect

Biochemical and Biophysical Research Communications

journal homepage: www.elsevier.com/locate/ybbrc

Intravital imaging of neutrophil recruitment in intestinal ischemia-reperfusion injury

Shintaro Hashimoto [a], Masaki Honda [a, *], Takayuki Takeichi [a], Masataka Sakisaka [a], Yasuko Narita [a], Daiki Yoshii [a], Keiichi Uto [a], Seisuke Sakamoto [a, b], Yukihiro Inomata [a, **]

[a] Department of Transplantation and Pediatric Surgery, Postgraduate School of Medical Sciences, Kumamoto University, Kumamoto, Japan
[b] National Center for Child Health and Development Organ Transplantation Center, Tokyo, Japan

ARTICLE INFO

Article history:
Received 27 November 2017
Accepted 22 December 2017
Available online 26 December 2017

Keywords:
Intravital microscopy
Transplantation
Inflammation
Innate immunity
Neutrophil
Intestinal ischemia-reperfusion injury

ABSTRACT

Background: Neutrophils are known to be key players in innate immunity. Activated neutrophils induce local inflammation, which results in pathophysiologic changes during intestinal ischemia-reperfusion injury (IRI). However, most studies have been based on static assessments, and few have examined real-time intravital neutrophil recruitment. We herein report a method for imaging and evaluating dynamic changes in the neutrophil recruitment in intestinal IRI using two-photon laser scanning microscopy (TPLSM).

Methods: LysM-eGFP mice were subjected to 45 min of warm intestinal ischemia followed by reperfusion. Mice received an intravenous injection of tetramethylrhodamine isothiocyanate-labeled albumin to visualize the microvasculature. Using a time-lapse TPLSM technique, we directly observed the behavior of neutrophils in intestinal IRI.

Results: We were able to image all layers of the intestine without invasive surgical stress. At low-magnification, the number of neutrophils per field of view continued to increase for 4 h after reperfusion. High-magnification images revealed the presence or absence of blood circulation. At 0–2 h after reperfusion, rolling and adhesive neutrophils increased along the vasculature. At 2–4 h after reperfusion, the irregularity of crypt architecture and transmigration of neutrophils were observed in the lamina propria. Furthermore, TPLSM imaging revealed the villus height, the diameters of the crypt, and the number of infiltrating neutrophils in the crypt. In the IRI group, the villus height 4 h after reperfusion was significantly shorter than in the control group.

Conclusions: TPLSM imaging revealed the real-time neutrophil recruitment in intestinal IRI. Z-stack imaging was useful for evaluating pathophysiological changes in the intestinal wall.

1. Introduction

Ischemia-reperfusion injury (IRI) of the intestine occurs in a variety of clinical conditions, including intestinal malrotation, strangulated ileus, superior mesenteric artery thrombosis, hemorrhagic shock, trauma, surgery, and transplantation [1]. The interruption of the blood supply results in ischemic injury that rapidly damages metabolically active tissues. Paradoxically, however, the restoration of the blood flow to the ischemic tissue initiates a cascade of events that can lead to additional cell injury, known as reperfusion injury [2,3].

Neutrophils, which are one of the earliest innate immune cells recruited to the sites of infection and inflammatory response, are crucial for the pathophysiology of IRI [4–8]. Neutrophils can cause tissue damage in several ways, including via the secretion of

Abbreviations: TPLSM, two-photon laser-scanning microscopy; IRI, ischemia-reperfusion injury; GFP, green fluorescent protein; ROS, reactive oxygen species; PBS, phosphate-buffered saline; TRITC, tetramethylrhodamine isothiocyanate; AST, aspartate aminotransferase; ALT, alanine aminotransferase; LDH, lactate dehydrogenase; SEM, standard error of the mean.

* Corresponding author. Department of Transplantation and Pediatric Surgery, Postgraduate School of Medical Sciences, Kumamoto University, 1-1-1 Honjo, Chuo-ku, Kumamoto 860-8556, Japan.
** Corresponding author. Department of Transplantation and Pediatric Surgery, Postgraduate School of Medical Sciences, Kumamoto University, 1-1-1 Honjo, Chuo-ku, Kumamoto 860-8556, Japan.
E-mail addresses: masakihonda0729@gmail.com (M. Honda), yino@kuh.kumamoto-u.ac.jp (Y. Inomata).

https://doi.org/10.1016/j.bbrc.2017.12.140
0006-291X/

proteolytic enzymes from cytoplasmic granules, neutrophil extracellular traps formation, and physical impairment of the microcirculation. Many neutrophils promote uncontrolled inflammation, and the depletion of redundant neutrophils is also implied to ameliorate tissue injury in various IRI models [9,10]. In intestinal IRI, the emigration of neutrophils from the postcapillary venules to areas of inflammation is a complex and highly coordinated process [11].

Thus far, the analysis of the status of neutrophils in intestinal IRI has been mainly based on the static assessment of histologic sections or an alternative index, such as myeloperoxidase activity, and few studies have analyzed the *in vivo*, real-time neutrophil recruitment. Therefore, the complexity and the dynamic features of the immune responses induced by neutrophils have been difficult to capture. We previously demonstrated the *in vivo* imaging of neutrophil recruitment in hepatic IRI using two-photon laser-scanning microscopy (TPLSM) [12,13]. TPLSM is one of the most progressive new developments in the field of imaging technology. It has numerous advantages over other modalities, including high-resolution, deep-site imaging, less phototoxicity, and less photobleaching than conventional confocal laser-scanning microscopy. These advantages are particularly useful for imaging tissues and organs in living beings [14–16].

In the present study, we present a method for examining neutrophil recruitment in intestinal IRI using TPLSM. We established our methodology by combining 1) a mouse intestinal IRI model, 2) LysM-eGFP transgenic mice, 3) the extension of the intestinal wall by phosphate-buffered saline (PBS) introduction and a tie technique, 4) butylscopolamine, 5) a stereotaxic device, and 6) TPLSM. With this novel method, we were able to visualize all of the layers of the intestine and analyzed the real-time neutrophil recruitment in live mice.

2. Materials and methods

2.1. Animals

LysM-eGFP mice were a generous gift from Dr. T. Graf (Center for Genomic Regulation, Barcelona, Spain). These mice express eGFP under the lysozyme M promoter, and their neutrophils are visualized by the expression of $eGFP^{hi}$ [17]. Mice were maintained in a specific-pathogen-free environment with free access to standard food and water throughout the experimental period at the Animal Resource Facility at Kumamoto University. Male LysM-eGFP mice at 8–12 weeks of age weighing 22–26 g were used for all experiments. The temperature was maintained at $22 \pm 2\,^{\circ}C$. All experiments were performed according to the guidelines of the Institutional Animal Committee of Kumamoto University.

2.2. Intestinal I/R injury model

Mice were anesthetized with an intraperitoneal injection of xylazine (10 mg/kg; Tokyo Kasei Kogyo, Tokyo, Japan) and ketamine (100 mg/kg; Fujita, Tokyo, Japan). After midline laparotomy, mice underwent a sham or I/R operation. In the I/R group, a part of the ileum supplied by a single branch of the superior mesenteric artery was exteriorized. Ligatures using 6-0 non-absorbable sutures were tightly applied to the marginal arteries and veins to prevent blood flow. An atraumatic microvascular clip (0.29 N; BEAR Medic; Tokyo, Japan) was placed across the superior mesenteric artery and vein, and the abdomen was closed. After 45 min of ischemia, the abdomen was reopened, and the clip was removed. Evidence of ischemia and reperfusion was confirmed by the intestinal color changes. In the control group, a sham operation was performed using the same protocol but without vascular occlusion. The mice were placed on a heating pad to maintain their body temperature at 37 °C throughout the procedure.

2.3. Intravital imaging of the intestine using TPLSM

Mice were prepared for intravital imaging using a protocol modified from previous reports [15,18,19]. After exteriorization of the target ileum, 0.5 mL of PBS was introduced into the collapsed ileum using a 30-G needle (Terumo Corporation, Tokyo, Japan) to visualize vertically all layers of the ileum, from the serosa to the mucosa. The exteriorized ileum was tied to the muscle layer of the abdomen using 6-0 non-absorbable sutures, and a 20-mm-diameter cover-ring was attached with glue. The ring was fixed into the arms of a stereotaxic holder. The hole of the ring was filled with PBS, and a cover-glass was placed onto the ring. General anesthesia was maintained with subcutaneous injections of xylazine (5 mg/kg) and ketamine (50 mg/kg) at 1- to 2-h intervals, and hydration was maintained by subcutaneous injections of 0.5 mL warmed saline every hour. The mice received an intravenous injection of tetramethylrhodamine isothiocyanate (TRITC)-labeled albumin (500 μg; Sigma-Aldrich, Tokyo, Japan) just prior to imaging to visualize the blood vessels. At the same time, butylscopolamine (0.2 mg/kg; Boehringer Ingelheim, Tokyo, Japan) was administered intravenously to minimize peristalsis of the intestine. Fig. 1A shows the intestinal preparation and setup of TPLSM for intravital imaging. The imaging system comprised a BX61WI upright microscope and FV1000MPE (Olympus, Tokyo, Japan) laser-scanning microscope system. In TPLSM mode, a Mai Tai HP Deep See femtosecond-pulsed laser (Spectra Physics, Santa Clara, CA, USA) was turned to and mode-locked at 840 nm. The intestine was scanned and fluorescence emission captured by the external non-descanned detectors (570-nm mirror and bandpass emission filters at 495–540 nm for eGFP and at 575–630 nm for TRITC). Time-lapse images were taken using the FV10-ASW version 3.0 software program (Olympus). For imaging at low-magnification, x-y planes spanning 1270×1270 μm at a resolution of 2.485 μm/pixel were imaged continuously at 1 frame every 1.644 s for 5–10 min using an Olympus UMPLFLN x10 W (numerical aperture, 0.30; working distance, 3.5 mm) objective lens. The intestine images were recorded hourly for 4 h at 37 frames/sec in the same position throughout imaging. For imaging at high-magnification, images were recorded using an Olympus XLPLN 25X WMP (water immersion; numerical aperture, 1.05; working distance, 2.0 mm) objective lens. High-magnification images were recorded by zooming in suitably to focus on the neutrophil morphology at the single-cell level.

2.4. Z-stack imaging of the intestinal wall

Using TPLSM, optical tomographic slices on the z-plane were obtained by moving the tomographic images on the x-y plane in the z-direction. Image stacks were collected at a 2-μm vertical step size from the serosa to the mucosa of the ileum. We calculated the villus height in the control and the IRI groups using z-stack imaging.

2.5. Image analyses

For analysis of the number of neutrophils, the TPLSM images were evaluated using the 'analyze and measure' command in the Image J software program (National Institutes of Health, Bethesda, MD, USA). Neutrophils were identified based on characteristics of fluorescent intensity (threshold of >50 in low-magnification imaging and 150 in high-magnification imaging) and cell size (5–15 μm). Under these conditions, neutrophils (GFP^{hi}) and monocytes/macrophages (GFP^{low} and larger than 20 μm) were differentiated based on their brightness levels and distinct

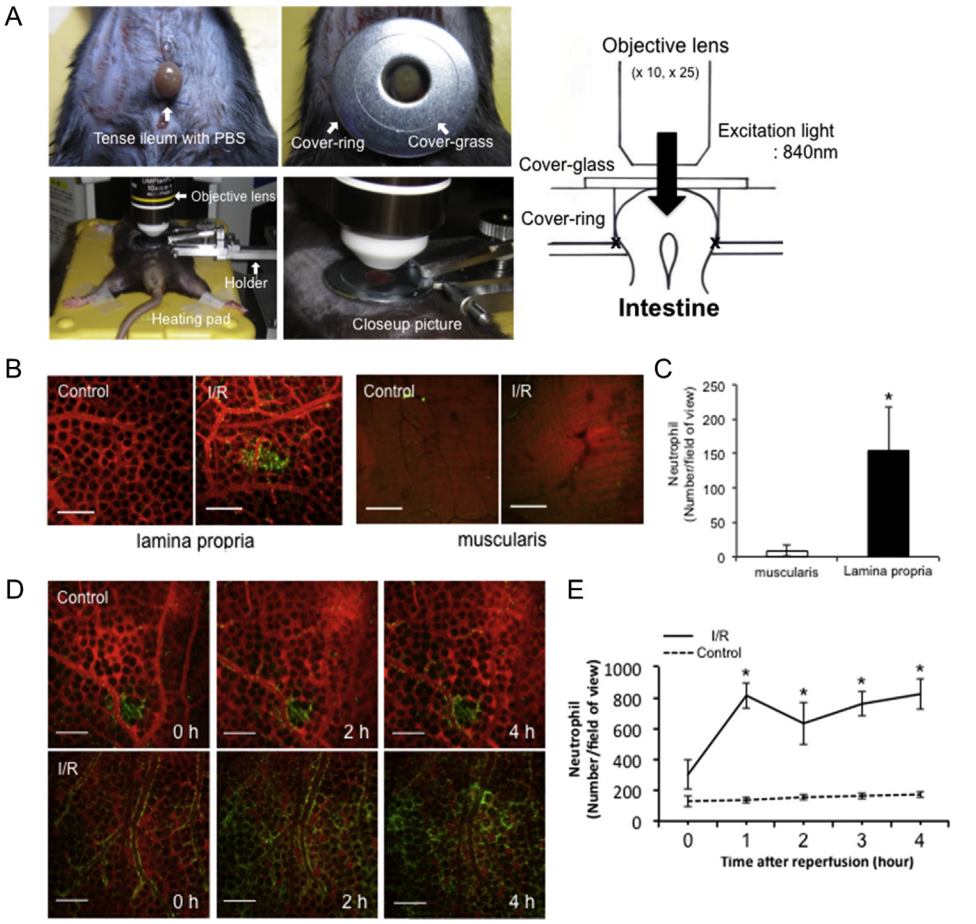

Fig. 1. Intravital imaging at low-magnification reveals the recruitment of neutrophils in intestinal IRI with wide range. (A) Setup for intravital imaging in the intestine using TPLSM. (B) Representative intestinal images of the control group and immediately after reperfusion at low-magnification. Scale bar = 200 μm. (C) The average number of neutrophils in the muscle layer and the lamina propria in the normal intestine. N = 5 per group. (D, E) Number of neutrophils per field of view in response to control operation or IRI. N = 5 per group. Error bars, SEM. *P < .01, compared with the control group. Scale bar = 200 μm.

morphologic characteristics. Three-dimensional (3D) reconstruction of z-stack imaging was performed using the Image J software program.

2.6. Histology

A part of the ileum subjected to IRI was removed, and samples were fixed in 10% buffered formalin and embedded in paraffin. Longitudinal sections of intestine (5 μm) obtained from the control and IRI groups were stained with hematoxylin and eosin. The park score at each time point was analyzed [20].

2.7. Assessment of the intestinal damage

Serum aspartate aminotransferase (AST), alanine aminotransferase (ALT), and lactate dehydrogenase (LDH) levels, which are all indicators of intestinal injury, were measured using a Hitachi 7180 auto-analyzer (Hitachi High-Technologies, Tokyo, Japan).

2.8. Statistical analyses

Data were expressed as the mean ± standard error of the mean (SEM). An unpaired Student's *t*-test or Mann-Whitney *U* test was used for comparisons between two groups, as appropriate. $P < .05$ was considered statistically significant. All tests were two-tailed. All statistical analyses were performed using the statistical package PASW Statistics 18 for Windows (IBM, Tokyo, Japan).

3. Results

3.1. Imaging of the intestine at low-magnification

We first imaged the intestine at low-magnification to establish a general view on TPLSM. Fig. 1B shows the TPLSM images of the intestinal lamina propria and muscle layer in the control and IRI groups immediately after reperfusion. The intestinal vasculatures were visualized with TRITC-albumin (red), and neutrophils were visualized with eGFP^{hi} (green). The images showed regularly aligned luminal crypt orifices and an ordered capillary network in the lamina propria. The crossover muscle fiber could be observed at the muscle layer, although there were no crypts. The average number of neutrophils in the muscle layer was significantly lower than that in the lamina propria in steady state (8.4 ± 7.99 vs. 154.4 ± 63.1, $P = .008$) (Fig. 1C). Time-lapse imaging (Supplementary Video 1) revealed the real-time movement of neutrophils in the intestine. In the control group, the number of neutrophils per field of view remained constant over 4 h at approximately 120. In the IRI group, the number gradually increased from 357.1 ± 140.2 to 838.2 ± 107.4, 705.8 ± 184.4, 758.2 ± 109.5, and 802.2 ± 139.9 at successive imaging time points over 4 h (Fig. 1D and E).

Supplementary video related to this article can be found at https://doi.org/10.1016/j.bbrc.2017.12.140

3.2. Imaging of the intestine at high-magnification

High-magnification images revealed the presence or absence of blood circulation in the intestine. In addition, we were able to observe clearly the movement of neutrophils at a single-cell level, such as flowing, tethering, rolling, adhering, or crawling to endothelium of the intestinal microvascular (Fig. 2A–C). At 0 h after reperfusion, the number of adhering neutrophils along the vasculature in lamina propria was increased compared with the control group (16.8 ± 5.38 vs. 1.2 ± 0.84, $P = .009$). At 4 h after reperfusion, neutrophils had adhered solidly to the endothelial cells and infiltrated into the pericryptal stroma and the interepithelial space of the crypts. Next, we examined the architecture of the crypts at high-magnification. The intestinal crypts in the lamina propria were distorted in shape and appeared irregular in size in the IRI group. The average diameter of the crypts at 4 h after reperfusion in the IRI group tended to be smaller than in the control group, albeit not significantly so (49.8 ± 3.24 vs. 52.1 ± 2.82 μm, $P = .079$) (Fig. 3A and B).

3.3. Effects of intestinal IRI on the infiltration of neutrophils into crypts

In the control group, few neutrophils were observed in the crypt at the lamina propria during imaging. In contrast, in the IRI group, the number of infiltrating neutrophils in the crypt increased gradually from 0 to 4 h after reperfusion (1.2 ± 0.79, 1.9 ± 0.74, 4.5 ± 1.43, 6.9 ± 1.97, 8.3 ± 1.64/crypt at 0, 1, 2, 3, and 4 h, respectively; Fig. 3C and D). The average number of crypts with a disrupted architecture per field of view was significantly higher in the IRI group than in the control group (3.8 ± 0.79 vs. 0.2 ± 0.42, $P < .001$).

3.4. Effects of intestinal IRI on the contraction of villus height

Z-stack TPLSM imaging enabled the investigation of the villus height (Supplementary Video 2). The 3D reconstruction of the z-stack imaging showed visual evidence of the morphological changes induced by IRI and the distribution of the accumulated neutrophils in the intestine (Fig. 4A and B). The villus height of the ischemic intestine at 4 h after reperfusion was significantly smaller than in the control group (107.6 ± 20.7 vs. 149.0 ± 25.2 μm, $P = .022$; Fig. 4C).

Supplementary video related to this article can be found at https://doi.org/10.1016/j.bbrc.2017.12.140

3.5. Histological and biochemical analyses of intestinal IRI

Histologically, the intestinal IRI group showed a higher Park score from 0 to 6 h after reperfusion than the control group (Fig. 4D and E). In addition, the intestinal IRI group showed a significant increase in the serum transaminase and LDH levels from 1 to 12 h after reperfusion compared with the control group (Fig. 4F–H). The trend in these data was similar to that of the intestinal injury severity determined by intravital TPLSM imaging.

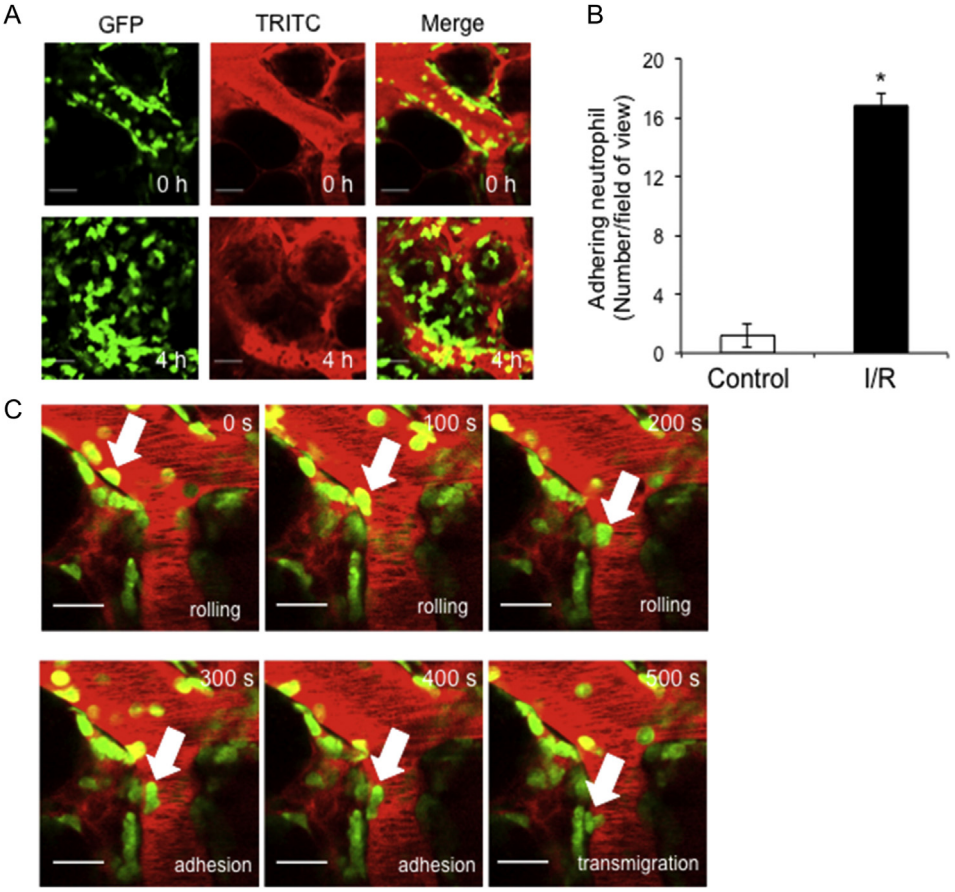

Fig. 2. Imaging at high-magnification reveals the distinct migratory patterns of neutrophils in intestinal IRI. (A) Imaging in the IRI group at 0 and 4 h after reperfusion in the lamina propria. Scale bar = 30 μm. (B) The average number of adhering neutrophils along the vasculature in the control group and at 0 h after reperfusion. N = 5 per group. (C) Time-lapse images of neutrophil recruitment. Arrows indicate the same neutrophils at different time points. Scale bar = 20 μm.

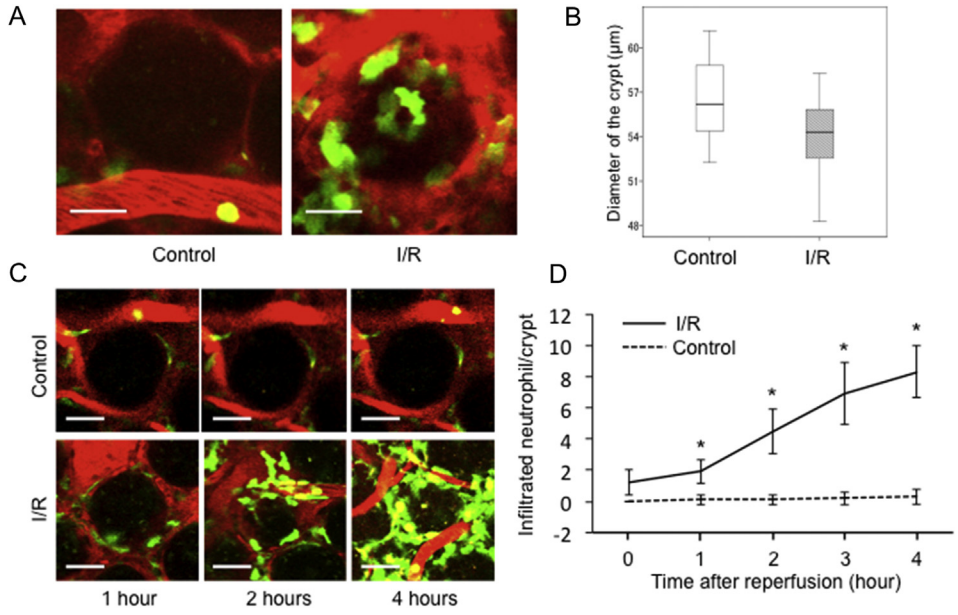

Fig. 3. Neutrophils infiltrate into the crypt and induce the morphological changes in intestinal IRI. (A) Imaging of the crypt architecture at high-magnification. (B) Box plot showing the crypt diameter in the control and IRI groups at 4 h after reperfusion. Two crypts were selected per mouse. N = 5 per group. (C) Representative images of the crypt and neutrophils during intestinal IRI. (D) The number of infiltrating neutrophils in the crypt increased gradually over 0–4 h after reperfusion. Scale bar = 20 μm. N = 5 per group. Error bars, SEM. *P < .01, compared with the control group.

4. Discussion

The application of TPLSM to intravital imaging to luminal organs, such as the respiratory tract, stomach, intestine, ureter, and bladder, is difficult due to those organs' spontaneous movement. To image these luminal organs, organ fixation using a suction window or glue has been applied, but imaging still remains technically difficult. When imaging the intestinal tract, intestinal peristalsis and difficulty with achieving flattening are serious problems. In the present study, we resolved these issues using a technique to extend the intestinal wall along with the administration of butylscopolamine and the application of a stereotaxic device. We successfully visualized the intravital distinct migratory patterns of neutrophils as well as the change in the intestinal structure of each layer, blood circulation, and the villus height obtained by 3D-reconstructed imaging.

TPLSM has become an indispensable tool for intravital imaging, as the technique provides high-resolution deep-site images and enables real-time long-term imaging [21,22]. These characteristics are extremely useful for assessing the dynamic pathological changes under functionally and physiologically intact cellular conditions. Using this technique, Mizuno et al. described the activities of extracellular signal-regulated kinase and protein kinase A in neutrophils in inflamed intestinal tissue [23], and Orzekowsky-Schroeder et al. demonstrated the utility of TPLSM for differentiating the cell types in the living colon [24]. These reports demonstrated valuable data by taking advantage of the unique features of TPLSM for intravital imaging of the intestine.

A previous study reported an influx of inflammatory cells, including polymorphonuclear leukocytes, into the injury site during the first 120 min after IRI [25]. Another study reported that neutrophils arrive within minutes of IRI, although their numbers decrease over 24 h [26]. These studies evaluated the influx of inflammatory cells using histologic analyses, and a similar pattern of neutrophil invasion was seen in our study. We showed that the number of neutrophils in the lamina propria increased in a time-dependent manner over 4 h after the I/R injury. At high-magnification, we were able to observe the movement of neutrophils clearly at a single-cell level. At 0 h after reperfusion, the number of adhering neutrophils along the vasculature increased significantly, and neutrophils infiltrated into the pericryptal stroma and the interepithelial space of the crypts by 4 h after reperfusion. Time-lapse TPLSM imaging enabled the evaluation of the consecutive pathophysiological changes that occurred in the intestine.

In addition, the information obtained by 3D visualization is clear at a glance; we therefore believe that 3D-reconstructed imaging is very persuasive. In the present study, we focused on the neutrophil recruitment and basic physiological status during intestinal IRI, including the morphological changes, with no biological intervention. Thus, further studies from a biological perspective are required for a more thorough elucidation of the innate and adaptive immune process in intestinal IRI.

Intestinal IRI is related to various abdominal surgeries and organ transplantation procedures. Such injury reduces the patient's survival due to bacterial translocation, systemic inflammation, intestinal necrosis, and multi-organ failure. Intravital imaging will be useful for investigations of therapeutic agent delivery and pharmacokinetics as well as the real-time examination of their direct efficacy in those settings [27]. Furthermore, the progressive development of fluorescent transgenic mice and reagents will enable the identification of many kinds of immune cell subsets and distinct anatomical structures. Monitoring immune cell behavior at a single-cell level using TPLSM has a broad range of applications. It will be also important to examine the cell-cell interactions in each immune cell subset, as this is indispensable for orchestrating effective immune responses. Understanding the complex involvement of the immune system in intestinal IRI will aid in the development of novel therapeutic strategies in severe situations, which will subsequently improve the outcomes of abdominal surgery and organ transplantation.

Our study has several limitations. First, motion artifacts of the imaging induced by intestinal peristalsis, breathing, and the heartbeat could not be completely suppressed. This was particularly important for imaging at high-magnification, although these

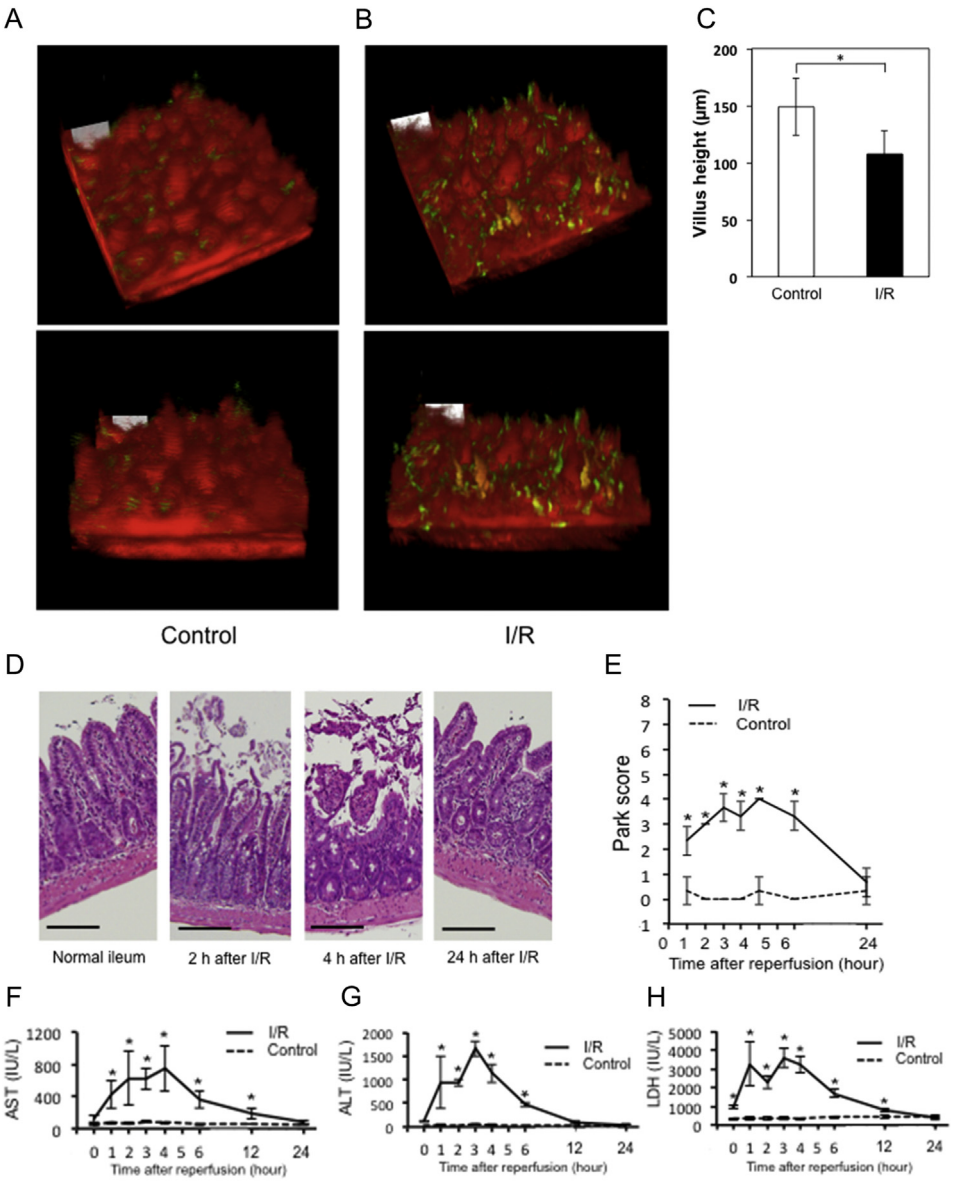

Fig. 4. The 3D reconstructed imaging is useful for evaluating pathophysiological changes of intestine during IRI. (A, B) Three-dimensional reconstruction of the z-stack intestinal TPLSM imaging. (C) The villus height of the control group and at 4 h after IRI. N = 5 per group. Error bars, SEM. *P < .01, compared with the control group. (D) Representative hematoxylin and eosin staining of the intestine including normal ileum, and ileum at 2, 4, and 24 h after IRI. (E) The transition of the park score in the control and IRI groups. (N = 3 per group. Error bars, SEM). The serum levels of (F) AST, (G) ALT, and (H) LDH were measured at 0, 1, 2, 3, 4, 6, 12, and 24 h after IRI (N = 5 per group. Error bars, SEM). *P < .01, compared with the control group.

artifacts were minimized using a stabilizing holder, additional anesthesia, and the administration of butylscopolamine. Second, surgical stress, exteriorization of the intestine, and its fixation might provoke intestinal microcirculatory disturbance. To overcome this problem, we focused on reducing these effects and confirmed that the color of the intestine had not been changed by the compression. A novel approach that reduces physiological changes and has deeper photon penetration and easier access to the intestine than conventional modalities is required.

In conclusion, TPLSM was successfully applied for intravital imaging of intestinal IRI. This method allowed for the evaluation of real-time neutrophil recruitment as well as the pathophysiological changes in the intestinal wall. Our findings will aid in the development of effective approaches to determining the mechanisms that underlie the immune responses in intestinal IRI.

Conflicts of interest

The authors declare no conflicts of interest.

Acknowledgements

This work was funded by grants from the Ministry of Education, Culture, Sports, Sciences and Technology of Japan (KAKENHI 26461918) and JSS Young Researcher Award (Japan Surgical Society). We thank Dr. T. Graf (Center for Genomic Regulation, Barcelona, Spain) for providing LysM-eGFP mice.

Transparency document

Transparency document related to this article can be found online at https://doi.org/10.1016/j.bbrc.2017.12.140.

References

[1] B. Vollmar, M.D. Menger, Intestinal ischemia/reperfusion: microcirculatory pathology and functional consequences, Langenbeck's Arch. Surg. 396 (2011) 13–29.

[2] C.D. Collard, S. Gelman, Pathophysiology, clinical manifestations, and prevention of ischemia-reperfusion injury, Anesthesiology 94 (2001) 1133–1138.

[3] E.E. Moore, F.A. Moore, R.J. Franciose, F.J. Kim, W.L. Biffl, A. Banerjee, The postischemic gut serves as a priming bed for circulating neutrophils that provoke multiple organ failure, J. Trauma 37 (1994) 881–887.

[4] S.D. Fleming, J. Anderson, F. Wilson, T. Shea-Donohue, G.C. Tsokos, C5 is required for CD49d expression on neutrophils and VCAM expression on vascular endothelial cells following mesenteric ischemia/reperfusion, Clin. Immunol. 106 (2003) 55–64.

[5] L.A. Hernandez, M.B. Grisham, B. Twohig, K.E. Arfors, J.M. Harlan, D.N. Granger, Role of neutrophils in ischemia-reperfusion-induced microvascular injury, Am. J. Physiol. 253 (1987) H699–H703.

[6] R. Schramm, H. Thorlacius, Neutrophil recruitment in mast cell-dependent inflammation: inhibitory mechanisms of glucocorticoids, Inflamm. Res. 53 (2004) 644–652.

[7] Y.Z. Lu, C.C. Wu, Y.C. Huang, C.Y. Huang, C.Y. Yang, T.C. Lee, C.F. Chen, L.C. Yu, Neutrophil priming by hypoxic preconditioning protects against epithelial barrier damage and enteric bacterial translocation in intestinal ischemia/reperfusion, Lab. Invest. 92 (2012) 783–796.

[8] E. Kolaczkowska, P. Kubes, Neutrophil recruitment and function in health and inflammation, Nat. Rev. Immunol. 13 (2013) 159–175.

[9] M. Abu-Amara, S.Y. Yang, N. Tapuria, B. Fuller, B. Davidson, A. Seifalian, Liver ischemia/reperfusion injury: processes in inflammatory networks–a review, Liver Transplant. 16 (2010) 1016–1032.

[10] A. Bonaventura, F. Montecucco, F. Dallegri, Cellular recruitment in myocardial ischaemia/reperfusion injury, Eur. J. Clin. Invest. 46 (2016) 590–601.

[11] I.H. Mallick, W. Yang, M.C. Winslet, A.M. Seifalian, Ischemia-reperfusion injury of the intestine and protective strategies against injury, Dig. Dis. Sci. 49 (2004) 1359–1377.

[12] M. Honda, T. Takeichi, K. Asonuma, K. Tanaka, M. Kusunoki, Y. Inomata, Intravital imaging of neutrophil recruitment in hepatic ischemia-reperfusion injury in mice, Transplantation 95 (2013) 551–558.

[13] M. Honda, T. Takeichi, S. Hashimoto, D. Yoshii, K. Isono, S. Hayashida, Y. Ohya, H. Yamamoto, Y. Sugawara, Y. Inomata, Intravital imaging of neutrophil recruitment reveals the efficacy of FPR1 blockade in hepatic ischemia-reperfusion injury, J. Immunol. 198 (2017) 1718–1728.

[14] G. Camirand, Q. Li, A.J. Demetris, S.C. Watkins, W.D. Shlomchik, D.M. Rothstein, F.G. Lakkis, Multiphoton intravital microscopy of the transplanted mouse kidney, Am. J. Transplant. 11 (2011) 2067–2074.

[15] K. Tanaka, Y. Koike, K. Matsushita, M. Okigami, Y. Toiyama, M. Kawamura, S. Saigusa, Y. Okugawa, Y. Inoue, K. Uchida, T. Araki, Y. Mohri, A. Mizoguchi, M. Kusunoki, Visualization of in vivo thromboprophylactic and thrombolytic efficacy of enoxaparin in laser-induced vascular endothelial injury model using multiphoton microscopy, Am. J. Transl. Res. 7 (2015) 79–87.

[16] D. Fiole, J.N. Tournier, Intravital microscopy of the lung: minimizing invasiveness, J. Biophot. 9 (2016) 868–878.

[17] N. Faust, F. Varas, L.M. Kelly, S. Heck, T. Graf, Insertion of enhanced green fluorescent protein into the lysozyme gene creates mice with green fluorescent granulocytes and macrophages, Blood 96 (2000) 719–726.

[18] Y. Toiyama, A. Mizoguchi, Y. Okugawa, Y. Koike, Y. Morimoto, T. Araki, K. Uchida, K. Tanaka, H. Nakashima, M. Hibi, K. Kimura, Y. Inoue, C. Miki, M. Kusunoki, Intravital imaging of DSS-induced cecal mucosal damage in GFP-transgenic mice using two-photon microscopy, J. Gastroenterol. 45 (2010) 544–553.

[19] K. Goto, G. Kato, I. Kawahara, Y. Luo, K. Obata, H. Misawa, T. Ishikawa, H. Kuniyasu, J. Nabekura, M. Takaki, In vivo imaging of enteric neurogenesis in the deep tissue of mouse small intestine, PLoS One 8 (2013), e54814.

[20] P.O. Park, U. Haglund, G.B. Bulkley, K. Falt, The sequence of development of intestinal tissue injury after strangulation ischemia and reperfusion, Surgery 107 (1990) 574–580.

[21] L. Dao, B. Glancy, B. Lucotte, L.C. Chang, R.S. Balaban, L.Y. Hsu, A model-based approach for microvasculature structure distortion correction in two-photon fluorescence microscopy images, J. Microsc. 260 (2015) 180–193.

[22] S. Ipponjima, T. Hibi, T. Nemoto, Three-dimensional analysis of cell division orientation in epidermal basal layer using intravital two-photon microscopy, PLoS One 11 (2016), e0163199.

[23] R. Mizuno, Y. Kamioka, K. Kabashima, M. Imajo, K. Sumiyama, E. Nakasho, T. Ito, Y. Hamazaki, Y. Okuchi, Y. Sakai, E. Kiyokawa, M. Matsuda, In vivo imaging reveals PKA regulation of ERK activity during neutrophil recruitment to inflamed intestines, J. Exp. Med. 211 (2014) 1123–1136.

[24] R. Orzekowsky-Schroeder, A. Klinger, B. Martensen, M. Blessenohl, A. Gebert, A. Vogel, G. Huttmann, In vivo spectral imaging of different cell types in the small intestine by two-photon excited autofluorescence, J. Biomed. Optic. 16 (2011) 116025.

[25] R. Hayward, A.M. Lefer, Time course of endothelial-neutrophil interaction in splanchnic artery ischemia-reperfusion, Am. J. Physiol. 275 (1998) H2080–H2086.

[26] C. Hierholzer, J.C. Kalff, G. Audolfsson, T.R. Billiar, D.J. Tweardy, A.J. Bauer, Molecular and functional contractile sequelae of rat intestinal ischemia/reperfusion injury, Transplantation 68 (1999) 1244–1254.

[27] G. Camirand, New perspectives in transplantation through intravital microscopy imaging, Curr. Opin. Organ Transplant. 18 (2013) 6–12.